Available online at www.sciencedirect.com

ScienceDirect

Geochimica et Cosmochimica Acta 197 (2017) 132–141

Geochimica et Cosmochimica Acta

www.elsevier.com/locate/gca

Europium and strontium anomalies in the MORB source mantle

Ming Tang *, William F. McDonough, Richard D. Ash

Department of Geology, University of Maryland, College Park, MD 20742, USA

Received 9 September 2015; accepted in revised form 18 October 2016; Available online 26 October 2016

Abstract

Lower crustal recycling depletes the continental crust of Eu and Sr and returns Eu and Sr enriched materials into the mantle (e.g., Tang et al., 2015, Geology). To test the hypothesis that the MORB source mantle balances the Eu and Sr deficits in the continental crust, we carried out high precision Eu/Eu^* and Sr/Sr^* measurement for 72 MORB glasses with MgO >8.5% from the Pacific, Indian, and Atlantic mid-ocean ridges. MORB glasses with MgO $\geqslant$ 9 wt.% have a mean Eu/Eu^* of 1.025 ± 0.025 ($2\ \sigma_m$, $n = 46$) and Sr/Sr^* of 1.242 ± 0.093 ($2\ \sigma_m$, $n = 41$) and these ratios are positively correlated. These samples show both positive and negative Eu and Sr anomalies, with no correlations between Eu/Eu^* vs. MgO or Sr/Sr^* vs. MgO, suggesting that the anomalies are not produced by plagioclase fractionation at MgO >9 wt.% and, thus, other processes must be responsible for generating the anomalies. We term these MORB samples primitive MORBs, as they record the melt Eu/Eu^* and Sr/Sr^* before plagioclase fractionation. Consequently, the mean oceanic crust, including cumulates, has a bulk Eu/Eu^* of ~1 and 20% Sr excess.

Considering that divalent Sr and Eu(II) diffuse faster than trivalent Pr, Nd, Sm, and Gd, we evaluated this kinetic effect on Sm–Eu–Gd and Pr–Sr–Nd fractionations during spinel peridotite partial melting in the MORB source mantle. Our modeling shows that the correlated Eu and Sr anomalies seen in primitive MORBs may result from disequilibrium mantle melting. Melt fractions produced during early- and late-stage melting may carry positive and negative Eu and Sr anomalies, respectively, that overlap with the ranges documented in primitive MORBs. Because the net effect of disequilibrium melting is to produce partial melts with bulk positive Eu and Sr anomalies, the MORB source mantle must have $Eu/Eu^* < 1.025 \pm 0.025$ ($2\ \sigma_m$) and $Sr/Sr^* < 1.242 \pm 0.093$ ($2\ \sigma_m$). Although we cannot rule out the possibility that recycled lower continental crustal materials, which have positive Eu and Sr anomalies, are partially mixed into the upper mantle (i.e., MORB source region), a significant amount of this crustal component must have been sequestered into the deep mantle, as supported by the negative $^{206}Pb/^{204}Pb$–Eu/Eu^* and $^{206}Pb/^{204}Pb$–Sr/Sr^* correlations in ocean island basalts.

Published by Elsevier Ltd.

Keywords: Eu anomaly; Sr anomaly; Primitive MORB; Disequilibrium melting; Lower crustal recycling

1. INTRODUCTION

Europium is present in two valence states (+2 and +3) in most magmatic systems. Europium(II) behaves like Sr^{2+} due to their similar ionic radii (1.25 vs. 1.26 Angstroms, respectively, Shannon, 1976). In the crust, where plagioclase is stable, Eu(II) and Sr are strongly partitioned into plagioclase and thus fractionated from Sm–Gd and Pr–Nd, respectively. During intra-crustal differentiation, Eu and Sr can be removed from the melt by fractional crystallization of plagioclase or retained in the residual plagioclase at the source. As a consequence, the upper continental crust is distinctly depleted in Eu and Sr while the lower continental crust possesses Eu and Sr excesses. The bulk continental crust likely has negative Eu and Sr anomalies based on observations of crustal samples (Rudnick and Gao,

* Corresponding author at: Earth Science Department, Rice University, Houston, TX 77005, USA.

E-mail address: tangmyes@gmail.com (M. Tang).

http://dx.doi.org/10.1016/j.gca.2016.10.025

0016-7037/Published by Elsevier Ltd.

2014; Tang et al., 2015), and most compositional models for the continental crust have negative Eu and Sr anomalies (Rudnick and Gao, 2014 and the references therein). Such Eu and Sr depletions in the crust likely result from lower crustal recycling.

Niu and O'Hara (2009) observed a positive correlation between Eu/Eu^* ($Eu/Eu^* = Eu_N/sqrt(Sm_N * Gd_N)$), Sr/Sr^* ($Sr/Sr^* = Sr_N/sqrt(Pr_N * Nd_N)$, CI1 normalizing data from Sun and McDonough (1989)) and MgO content in MORB samples from the East Pacific Rise. They also observed that the primitive MORB samples (MgO >9 wt.%) all have positive Eu and Sr anomalies (Eu/Eu^* and $Sr/Sr^* > 1$), and thus the depleted MORB mantle (DMM, the source region of MORB) might host the Eu and Sr that are missing from the continental crust. More recently, Arevalo and McDonough (2010) failed to reproduce the correlation between Eu/Eu^* and MgO in their global MORB dataset, which shows a large variation in Eu/Eu^* for MORB samples having MgO contents >9 wt.%. Similarly, both positive and negative Eu and Sr anomalies were observed in global primitive MORB by Jenner and O'Neill (2012a) and Gale et al. (2013). However, none of these studies were dedicated to high precision measurement of Eu/Eu^* and Sr/Sr^* in MORB. The total variation of Eu/Eu^*, in particular, is limited in primitive MORB and requires instrumental fractionation to be well calibrated for accurate measurement of Eu/Eu^*. To investigate this issue further, we developed a new LA-ICP-MS method (Tang et al., 2014), and measured Eu/Eu^* as well as Sr/Sr^* at high precision and accuracy in 72 primitive MORB glasses globally. In contrast to Niu and O'Hara's observations, our data show much reduced average Eu excesses in the primitive MORBs.

Europium and Sr anomalies in mantle partial melts may not be directly used to approximate Eu/Eu^* and Sr/Sr^* in the source. Experimental studies showed that the divalent Eu and Sr diffuses orders of magnitude faster than the trivalent Pr, Nd, Sm and Gd in clinopyroxene (Sneeringer et al., 1984; Van Orman et al., 2001; Cherniak and Liang, 2007). Disequilibrium melting in the MORB source mantle may result in Eu and Sr enrichments in the partial melts because Eu and Sr are preferentially extracted relative to Pr, Nd, Sm and Gd. In the second part of this work, we evaluate the degrees of Sm–Eu–Gd and Pr–Sr–Nd fractionations and consequent Eu/Eu^* and Sr/Sr^* generated by partial melting of an anomaly free source. Our calculation suggests that the MORB source mantle may have much less Eu and Sr excesses (permissively no Eu and Sr anomalies) than the primitive MORB.

2. SAMPLES AND ANALYTICAL METHODS

A total of 72 MORB glasses from 21 sites (Fig. 1) were measured for their Eu/Eu^*, Sr/Sr^* and MgO contents. Of these samples, 28 are from the Pacific, 22 are from the Indian and 22 are from the Atlantic. All samples have MgO contents >8.5%, and are thus relatively primitive. Eu/Eu^* and Sr/Sr^* were normalized to chondrite values from Sun and McDonough (1989).

The LA-ICP-MS method provides a better approach to evaluate Eu and Sr anomalies in MORB glasses than the solution ICP-MS method in that one can easily detect and avoid micro-crystals within the glass. The plagioclase micro-crystals, either crystalized from or assimilated into the melt, can significantly bias the measurements of Eu and Sr anomalies. The LA-ICP-MS data reduction method in (Tang et al., 2014) was adopted from Liu et al. (2008), and allows simultaneous determination of major and trace element concentrations in volatile-free samples. One of the two basaltic reference materials, KL2-G and BIR-1G, was analyzed after every one or two samples (see Supplementary file for measurements on reference materials). A long-term reproducibility of ~3% (2 SD) was achieved for both Eu/Eu^* in KL2-G and BIR1-G. The Eu/Eu^* measured in reference materials over a wide range of compositions agree with GeoReM preferred values (http://georem.mpch-mainz.gwdg.de/) within 3%. To avoid potential heterogeneities such as micro-crystals, we measured each glass chip three to four times at different sites (see Supplementary file for data). The uncertainties for BHVO-2G, our calibration standard, are ~2% (2 RSD) for Eu/Eu^* and ~8% (2 RSD) for Sr/Sr^*. We excluded individual spot analyses having distinct Eu/Eu^* (>2 SD reproducibility different from the remainder) or major element composition compared to the remainder of the analyses on the same sample, and took the average values of the remainder as the Eu/Eu^* and MgO content for each sample. The Sr/Sr^* were measured separately on the same set of samples using BHVO-2G as the calibration standard. Each sample was measured twice. Our repeated measurements of BIR-1G throughout the analytical session gave an average Sr/Sr^* of 3.44 ± 0.12 (2 SD, 2 RSD = 3.6%, $n = 15$), which agrees with the GeoReM preferred value within 2%. For Eu/Eu^*, twenty-five analyses (marked in red in the Supplementary file) were thus discarded from the total of 320 analyses (7.8% of the population). We compared the long-term reproducibility of the two reference materials, and standard deviation of multiple analyses of each sample, and took whichever is greater as the uncertainty. Nineteen randomly selected samples were re-analyzed on different days to check the reproducibility of Eu/Eu^* measurements (see Supplementary file for the plot). One possible caveat with our approach is that our MORB glass chips are small, mostly several mm^3 volumes. How representative are these glass chips compared to those chunks of whole rocks remains to be investigated.

3. RESULTS

The primitive MORB samples we analyzed show both positive and negative Eu ($Eu/Eu^* = 0.92–1.13$) and Sr anomalies ($Sr/Sr^* = 0.81–1.98$) (Fig. 2). No significant correlations between Eu/Eu^* (or Sr/Sr^*) and MgO when MgO exceeds 8.5%, precluding the extrapolation of Niu and O'Hara's putative trend to higher MgO. Plagioclase saturates at around 9 wt.% MgO (Bender et al., 1984; Niu et al., 2002; Niu and O'Hara, 2009) and its fractional crystallization only happens within the oceanic crust (Wanless and Shaw, 2012). The three ocean basins, Pacific, Indian, and Atlantic, show no discernable difference in their mean Eu/Eu^* (1.011 ± 0.013, 1.023 ± 0.020 and 1.030 ± 0.024,

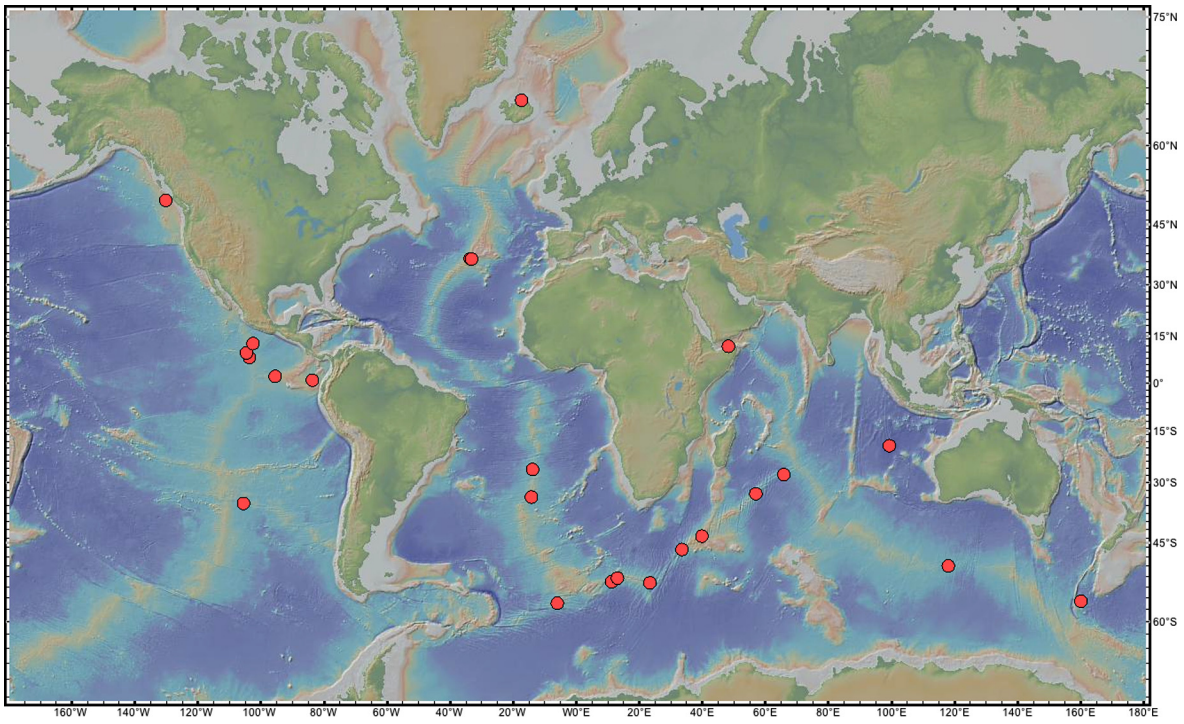

Fig. 1. Sample locations (red circles) of the MORB glasses analyzed in this study. (For interpretation of the references to colour in this figure legend, the reader is referred to the web version of this article.)

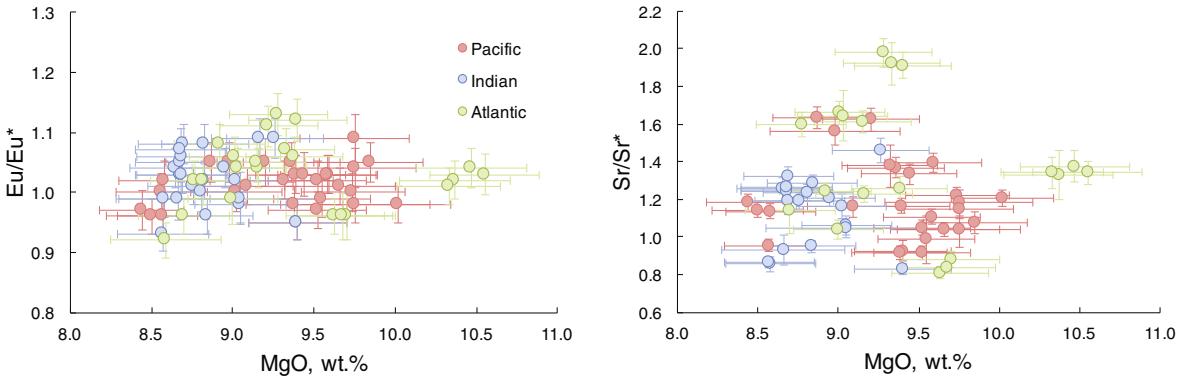

Fig. 2. Eu/Eu* and Sr/Sr* vs. MgO in primitive MORB glasses analyzed in this study. Error are 2 σ. See text for more details on uncertainty evaluation.

respectively) and Sr/Sr* (1.19 ± 0.08, 1.14 ± 0.08, 1.38 ± 0.16) at two standard error level.

The full dataset yields mean Eu/Eu* of 1.020 ± 0.011 (2 σ_m, n = 72) and Sr/Sr* of 1.23 ± 0.07 (2 σ_m, n = 64). Samples with MgO < 9% were filtered out to minimize the effect of plagioclase fractionation. The remaining samples yield mean Eu/Eu* of 1.025 ± 0.013 (2 σ_m, n = 46) and Sr/Sr* of 1.24 ± 0.09 (2 σ_m, n = 41), which are not different from the full dataset mean. Considering uncertainties for the Eu/Eu* and Sr/Sr*, global primitive MORBs (MgO >9%) have mean Eu/Eu* of 1.025 ± 0.025 (2 σ_m) and Sr/Sr* of 1.24 ± 0.14 (2 σ_m). The method used to calculate Sr anomalies here enables direct comparison of our results with previous studies (e.g., Niu and O'Hara, 2009), but this method artificially introduces percent level positive Sr anomalies to depleted MORB samples with convex LREE curves. Therefore, the calculated mean Sr/Sr* may slightly overestimate the amount of Sr excess in primitive MORBs.

Our mean Eu/Eu* and Sr/Sr* for global MORBs with MgO >9% are consistent with results from Jenner and O'Neill (2012a) and Gale et al. (2013). (Fig. 3). The repeated analysis of Eu/Eu* in USGS standard BCR-2G by Jenner and O'Neill (2012b) is 5% higher than the GeoReM preferred value, which may account for their offset to higher average Eu/Eu* derived for high MgO MORBs (Fig. 3). The mean Eu/Eu* for primitive MORBs from this study, Jenner and O'Neill (2012a) and Gale et al. (2013) is lower than that reported by Niu and

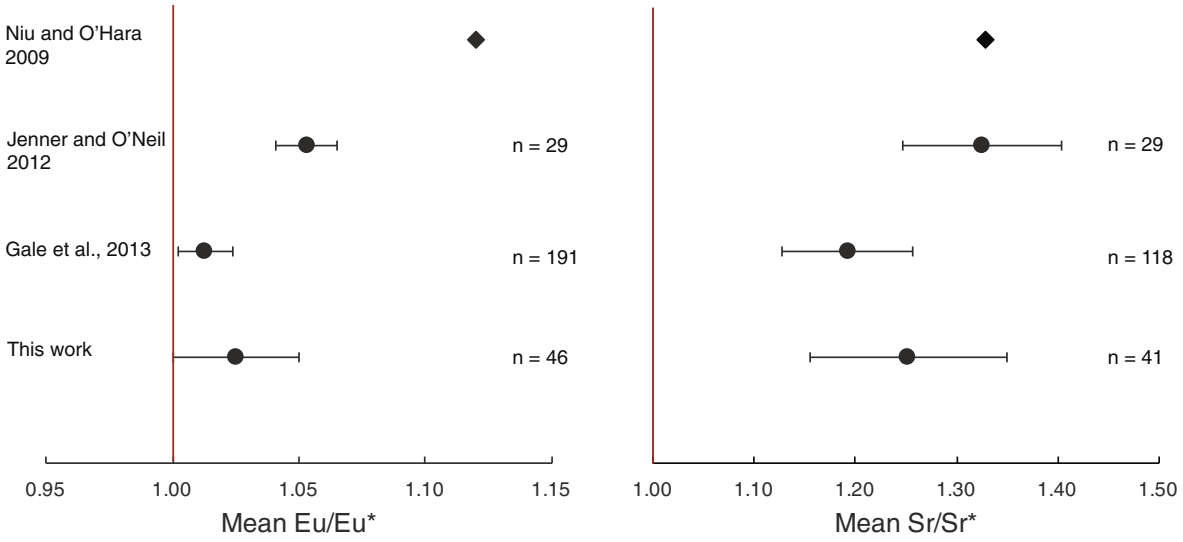

Fig. 3. Mean Eu/Eu* and Sr/Sr* measured in MORB with >9 wt.% MgO from this study compared with published estimates. Gale et al.'s (2013) data are from their own analyses plus their compilation, while the mean Eu/Eu* values from Niu and O'Hara (2009) and Jenner and O'Neill (2012a,b) are based their own analyses of MORB. Error bars are 2 σ_m.

O'Hara (2009). Niu and O'Hara's mean Eu/Eu* value was estimated using a set of local samples from the East Pacific Rise, and their detailed sample information was not provided.

4. DISCUSSION AND MODELING

4.1. The MgO criterion

Here we followed Niu and O'Hara (2009) and use MgO content as a filter during sample selection. Primitive MORB samples are non-existent since fractional crystallization readily occurs at mantle depths beneath mid ocean ridges (Wanless and Shaw, 2012). However, the early crystallizing phases olivine and spinel have no effect on Eu/Eu* in the melts, which is only sensitive to plagioclase fractionation. Therefore, MORB samples undersaturated in plagioclase should represent the primitive Eu/Eu* of the source. Although plagioclase contains little MgO, co-crystallization of olivine and plagioclase produces positive correlations between MgO and plagioclase crystallization indices such as Sr/Sr* and Eu/Eu* (e.g., Niu and O'Hara, 2009; Jenner and O'Neill, 2012a; Gale et al., 2013). These observations justify the use of the MgO content as a criterion in selecting samples that can represent the primitive/bulk Eu/Eu* and Sr/Sr*.

Interaction with plagioclase cumulates in the lower oceanic crust can potentially alter Eu/Eu* and Sr/Sr* in the MORB melts. Despite the complexities of such cumulate-melt interaction, high MgO (>9%) MORB melts are mostly undersaturated in plagioclase, and would, thus, tend to dissolve plagioclase in the cumulates. Chemical re-equilibration may also happen during cumulate-melt interaction. In this process, Eu(II), which diffuses faster than Sm (III) and Gd(III) (Cherniak and Liang, 2007), is more likely to diffuse from plagioclase to the high MgO melts because cumulates on average are in equilibrium with the upper oceanic crust that is more evolved and has a higher Eu concentration than primitive MORB (see Supplementary file for Eu concentration vs. MgO in MORB). The net effect of either plagioclase dissolution or chemical re-equilibration is to increase the average Eu/Eu* in the high MgO melts during ascent through the crystal mush. The same effect applies to the Pr–Sr–Nd system. Therefore, primitive melts may have had even lower Eu/Eu* and Sr/Sr* values than our high MgO MORB samples, depending on the extent of cumulate-melt interaction.

Recycled oceanic crust can produce silica-rich melts that react with peridotite to form pyroxenite (Sobolev et al., 2005). Partial melting of pyroxenite in the mantle may produce melts with lower MgO contents than those of peridotite (Lambart et al., 2013). Pyroxenite-derived melts have been estimated to contribute between 10–30% by mass to MORB melts (Sobolev et al., 2007). Assuming peridotite-derived melts have primitive MgO contents >11% (the most primitive MORB sample analyzed here has 10.5% MgO), mixing pyroxenite- and peridotite-derived melts does not generate MORB with MgO < 9%, even assuming incorporation of a maximum of 30% pyroxenite-derived melts with ~4% MgO. Therefore, our MgO filter (>9%) may include primitive MORB samples with significant contributions from recycled crust in their source regions.

4.2. Modeling Sm–Eu–Gd and Pr–Sr–Nd fractionation during mantle melting

Both Eu and Sr anomalies are present in many primitive MORB samples. Here we show how kinetic + equilibrium effects that occur during partial melting of spinel peridotite can fractionate Eu from Sm and Gd, and Sr from Pr and Nd, leading to variations in Eu/Eu* and Sr/Sr* of MORB. Since kinetic effects cannot be evaluated by classic melting

models such as batch and equilibrium melting models, we will not consider these models in the following discussion. Europium(II), like Sr(II), is slightly more incompatible than Sm and Gd (see Table 1), which will lead to a slight enrichment of Eu relative to Sm and Gd during partial melting. In addition, Eu(II) and Sr diffuse faster than Sm–Gd and Pr–Nd, which may lead to significant fractionation (Cherniak and Liang, 2007), depending on the degree of disequilibrium melting. The dynamic melting model considered below is developed from Qin (1992). A list of parameters and their definitions is given in Table 2. We ignored the density difference between the melt and solid phases, as this will not affect the calculated mass ratios such as Eu/Eu^* and Sr/Sr^*.

Assumptions:

(1) Eu(II) has the same partition and diffusion coefficients as Sr.
(2) The MORB source has the mineral assemblage: 51.3% olivine (ol) + 34.1% orthopyroxene (opx) + 13.1% clinopyroxene (cpx) + 1.5% spinel (spl) (Niu, 1997).
(3) The following melting reaction occurs: 0.466 cpx + 0.652 opx = 0.167 ol + 1 melt (Niu, 1997).
(4) The melting temperature is 1300 °C.
(5) 20% partial melting occurs over the timescale of 1 Ma–100 Ma.
(6) Eu(II) fraction is 10–30%.
(7) For the diffusion calculations, all cpx and opx crystals are assumed to be spherical and have an initial radius of 3 mm.
(8) The porosity of the mantle remains at 1% during partial melting.
(9) The melts are rapidly extracted once the melt fraction exceeds the porosity, and are chemically separated from the residue.

We discuss the rationale for these assumptions next.

Diffusivity of pure Eu(II) has not yet been reported. However, under reducing conditions, Eu diffuses over an order of magnitude faster than under oxidizing conditions (Cherniak and Liang, 2007). Here we used the diffusivity of Sr (Sneeringer et al., 1984), which is up to three orders of magnitude faster than those of most REEs, to approximate that of Eu(II) (Table 1). The results of the model presented below change only a few percent when using a lower estimate of Eu(II) diffusivity (1.5 orders of magnitude faster than Sm and Gd).

The average relative melting rate, estimated using spreading rate, is on the order of 10^{-7}–10^{-8} yr^{-1} (or 3×10^{-4}–3×10^{-5} $kg/m^3/yr$). The instantaneous melting rate may have greater variability. Faster melting promotes greater Sm–Eu–Gd fractionation as long as the melt remains in equilibrium with the residue for Eu(II) (i.e., melting rate $<\sim 10^{-4}$ yr^{-1}). In Iceland, the estimated melting rate ranges from 10^{-6} to 10^{-8} yr^{-1}, possibly influenced by pressure release caused by deglaciation (Jull and McKenzie, 1996). Crowley et al. (2015) also found a link between glacial cycles at the surface and mantle melting at depth along mid-ocean ridges in Iceland and observed that glacial cycles drive variations in the production of oceanic crust. The samples with the largest positive Eu ($Eu/Eu^* = 1.07$–1.13) and Sr ($Sr/Sr^* = 1.91$–1.98) anomalies in our dataset are from Iceland or nearby ridge segments.

The fraction of Eu(II) depends on oxygen fugacity and the standard redox potential (Schreiber, 1986), the latter of which is dependent upon the composition of the system. Traditionally, $Eu(II)/Eu_{total}$ in MORB is approximated using plagioclase-melt Sr–Eu partition coefficients. Since partition coefficients are sensitive to composition, temperature and pressure, the calculated Eu(II) fraction shows significant variation in the literature. The early work by Sun et al. (1974) indicated 8–13% Eu(II) in mid-ocean ridge basalts. Aigner-Torres et al. (2007) determined 5–15% Eu (II) in a Pacific MORB sample under the quartz-magnetite-fayalite (QFM) buffer. More recently, Laubier et al.'s (2014) partition coefficient data showed that, in MORB, Eu(II) decreases from ~20% at QFM to ~12% at the nickel–nickel oxide (NNO) buffer. The oxygen fugacity at the top of the upper mantle falls within ±2 log units of the QFM buffer, and is heterogeneous on a small scale (Frost and McCammon, 2008). By measuring $Fe^{3+}/\Sigma Fe$ ratios in MORB glasses, Bézos and Humler (2005) and Cottrell and Kelley (2013) estimated that MORB oxygen fugacity is buffered at ~QFM. Based on Fe_2O_3 systematics during partial melting, Bézos and Humler (2005) further

Table 1
Partition coefficients and diffusion coefficients used in the model.

	Partition coefficients[a]		Diffusion coefficients (cm^2/s)	
	cpx	opx	cpx[b]	opx[c]
Pr	0.23	0.013	$3.8 * 10^{-16}$	$4.2 * 10^{-16}$
Sr	0.26	0.016	$1.9 * 10^{-12}$	$1.3 * 10^{-14}$
Nd	0.29	0.016	$4.0 * 10^{-16}$	$4.2 * 10^{-16}$
Sm	0.35	0.023	$5.3 * 10^{-16}$	$4.2 * 10^{-16}$
Eu(II)[d]	0.26	0.0036	$1.9 * 10^{-12}$	$1.3 * 10^{-14}$
Eu(III)	0.38	0.0286	$8.4 * 10^{-16}$	$4.2 * 10^{-16}$
Gd	0.41	0.036	$1.2 * 10^{-15}$	$5.8 * 10^{-16}$

[a] From Niu et al. (1996) except for Eu(II).
[b] Taken or interpolated from Van Orman et al. (2001) and Sneeringer et al. (1984).
[c] From Cherniak and Liang (2007); Sr diffusion coefficient in opx was approximated by Eu diffusion coefficient measured in air.
[d] Partition coefficients and diffusion coefficients of Eu(II) are assumed to the same as Sr due to the similarity between the two elements.

Table 2
Notation used in modeling.

Variable	Description	Unit
α	Ratio of melt extraction rate to melting rate	
C_j^i	Concentration of element i in mineral j	g/g
C_a^i	Concentration of element i in aggregated melt	g/g
C_r^i	Concentration of element i in residual melt	g/g
D_j^i	Diffusion coefficient of element i in mineral j	cm^2/s
f_j	Initial proportion of mineral j	
F	Melting degree	
K_j^i	Partition coefficient of element i between melt and j	
R_j	Radius of mineral j	cm
r_j	Distance to the crystal center of mineral j	cm
t	Time	s
V_j	Volume of mineral j	cm^3
V_a	Volume of aggregated melt	cm^3
V_r	Volume of residual melt	cm^3
ω_e	Melt extraction rate	cm^3/s
ω_m	Melting rate	cm^3/s
ω	Relative/normalized melting rate	yr^{-1}
X_j	Reaction coefficient of mineral j during melting	
φ	Porosity at the source	

proposed a fO_2 of QFM-1 for the MORB source region. Recently, the oxidation state of Eu in silicate melts was directly measured by X-ray absorption near edge structure (XANES) (Burnham et al. (2015). According to their empirical equation for Eu(III)/Eu_{total} as a function of oxygen fugacity, melt composition and temperature, the Eu(II) fraction is 20–30% in MORB melts. Given the above observations, we explored the Sm–Eu–Gd fractionation during partial melting by assuming 10–30% Eu(II) in the MORB source mantle. Less Eu(II) translates into a smaller Eu anomaly.

In our model, we considered only diffusion in clinopyroxene (cpx) and orthopyroxene (opx) to control the REE budgets in spinel peridotites. Following Qin (1992), we assume all crystals are spherical, the redistribution of the element concentration (C) within the crystals is controlled by volume diffusion:

$$\frac{\partial C_j^i}{\partial t} = D_j^i\left(\frac{\partial^2 C_j^i}{\partial r_j^2}+\frac{2}{r_j}\frac{\partial C_j^i}{\partial r_j}\right), 0 \leqslant r_j \leqslant R_j(t); j = \text{cpx, opx};$$
$$i = \text{Eu(II), Eu(III), Sm, Gd, Sr, Pr, Nd} \quad (1)$$

Three initial conditions are assumed:

(1) All minerals are initially homogeneous

$$\frac{\partial C_j^i|_{t=0}}{\partial r_j} = 0, 0 \leqslant r_j \leqslant R_j|_{t=0} \quad (2)$$

(2) Clinopyroxene and orthopyroxene are in equilibrium before melting

$$\frac{C_{\text{cpx}}^i|_{t=0}}{K_{\text{cpx}}^i} = \frac{C_{\text{opx}}^i|_{t=0}}{K_{\text{opx}}^i} \quad (3)$$

Two boundary conditions are:

(1) There is no chemical gradient in the center of the crystals

$$\frac{\partial C_j^i}{\partial r_j}|_{r_j=0} = 0 \quad (4)$$

(2) The crystal rims maintain equilibrium with the melt

$$C_j^i|_{r_j=R_j} = K_j^i C_r^i \quad (5)$$

Our modeling here follows Qin (1992), where he observed that disequilibrium effects are enhanced due to differences in relative diffusivities of highly incompatible elements. The concentrations (ppm) of an element i in the residual (C_r^i) and aggregated (C_a^i) melt are given by the two equations below, respectively:

$$\frac{d(V_r C_r^i)}{dt} = -\frac{d}{dt}\left\{\sum_j f_j \int_0^{R_j} 4\pi r_j^2 C_j^i dr_j\right\} - \omega_e C_r^i \quad (6)$$

$$C_a^i = \frac{1}{V_a}\left\{-\left[\sum_j\left(f_j\int_0^{R_j} 4\pi r_j^2 C_j^i dr_j\right) - \sum_j\left(f_j\int_0^{R_j|_{t=0}} 4\pi r_j^2 C_j^i dr_j\right)\right] - V_r C_r^i\right\} \quad (7)$$

The radius of mineral j is given by:

$$R_j = R_j|_{t=0}\sqrt[3]{1-\frac{X_j}{f_j}\omega t} \quad (8)$$

X_j used in the third assumption and here is the reaction coefficient of mineral j during melting.

$$\frac{dV_r}{dt} = \omega_m - \omega_e = \omega_m(1-\alpha) \quad (9)$$

$$\frac{dV_a}{dt} = \alpha\omega_m \quad (10)$$

$$\alpha = 0, \text{ when } F \leqslant \varphi; \quad (11a)$$

$$\alpha = \frac{1}{(1-\varphi)}, \text{ when } F > \varphi \quad (11b)$$

$$F = \omega t \quad (12)$$

As shown in Fig. 4, Eu and Sr are always enriched over Sm–Gd and Pr–Nd, respectively, in aggregated melts from spinel peridotite. The extent of Sm–Eu–Gd and Pr–Sr–Nd fractionations rapidly decrease with increasing degree of melting, and greater fractionations are produced under faster melting rates. The positive Eu (up to 1.13) and Sr (up to 1.98) anomalies in our primitive MORB samples can be produced by disequilibrium melting of an anomaly-free source under upper mantle melting conditions (Fig. 4). Fig. 5 plots Sr/Sr^* vs. Eu/Eu^* in aggregated melts as a function of Eu^{2+} fraction and melting rate, and it shows that disequilibrium melting of the MORB source mantle can produce positively correlated Sr/Sr^*–Eu/Eu^* in the melts, which mimics the mixing trends between the Depleted Mantle and recycled lower crust. The slope of Sr/Sr^*–Eu/Eu^* is sensitive to the Eu^{2+} fraction in the mantle source, and our data suggest that the mantle source has 10–20% of total Eu as Eu^{2+}. Future studies on Eu^{2+}/Eu^{3+} in peridotite may

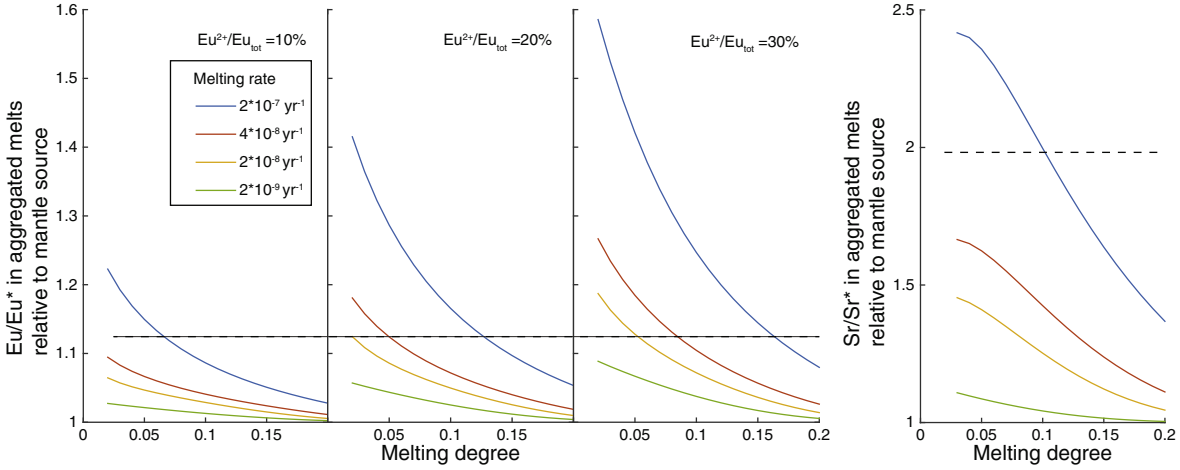

Fig. 4. Eu/Eu* and Sr/Sr* in aggregated melts as a function of Eu(II) fraction, melting rate in fraction/year and melting degree. The colors of the curves indicate melting rates. The gray dashed lines indicate the maximum positive Eu and Sr anomalies in the data reported here for primitive MORB. (For interpretation of the references to colour in this figure legend, the reader is referred to the web version of this article.)

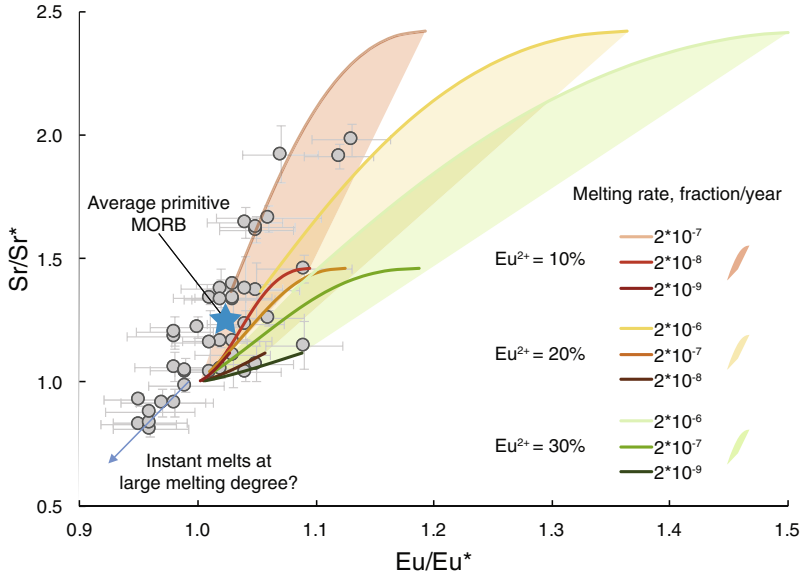

Fig. 5. Sr/Sr* vs. Eu/Eu* in primitive MORBs (MgO >9 wt.%) compared with calculated melt composition trajectories (2–20% partial melting).

help to clarify the significance of crust-mantle mixing vs. disequilibrium melting. Because partial melting of any extent of disequilibrium preferentially extracts Eu and Sr from the source, the residual assemblage will have progressively more negative Eu and Sr anomalies (Fig. 6). Thereby, later melts derived from residual peridotite that has experienced large degrees of melting can be depleted in Eu and Sr.

The Sm–Eu–Gd and Pr–Sr–Nd systematics in primitive MORB may be further complicated by interactions between melts and lower crustal cumulates during melt transport (Wanless and Shaw, 2012), as discussed above. Although magmatic processes can fractionate Eu from Sm–Gd, and Sr from Pr–Nd, mixing of melts generated at various depths and melting degrees tends to reduce the kinetic effects seen in the aggregated melts. Taking the disequilibrium melting effect into account, the MORB source mantle should have Eu/Eu* and Sr/Sr* less than average primitive MORBs, i.e., 1.025 ± 0.025 ($2\ \sigma_m$) and 1.242 ± 0.093 ($2\ \sigma_m$), respectively. For instance, if we assume the oceanic crust represents an average 10% melting product of the underlying mantle (Plank et al., 1995) and an average total melting timescale (melting from 0–20%) of 10 Ma (or $\sim 6.6 \times 10^{-5}$ kg/m^3/yr), the MORB mantle source would have Eu/Eu* and Sr/Sr* of 0.96–1.00 and 0.99, respectively. To test further disequilibrium melting effects produced during mantle partial melting, we suggest future work on high precision measurements of Eu/Eu* and Sr/Sr* in peridotitic clinopyroxenes (the major host for the REE and Sr). The

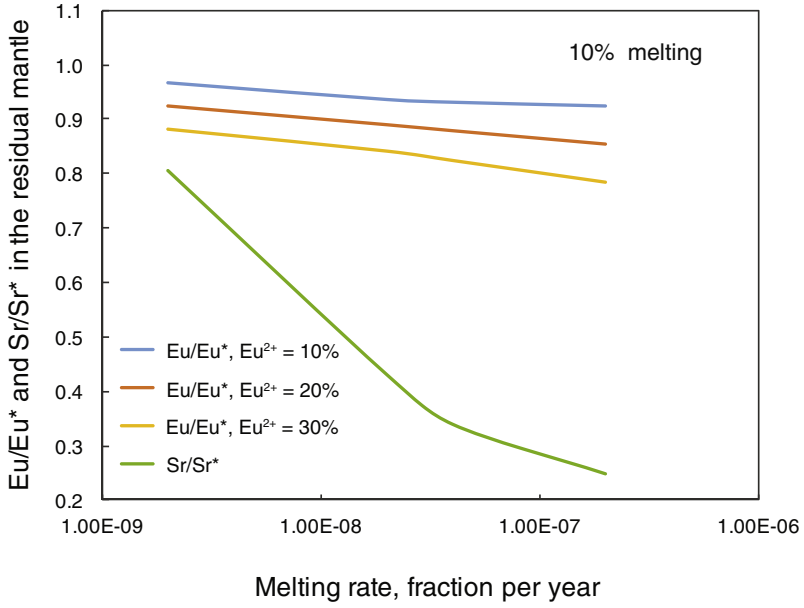

Fig. 6. Eu/Eu* and Sr/Sr* in the mantle residue after 10% degree melting.

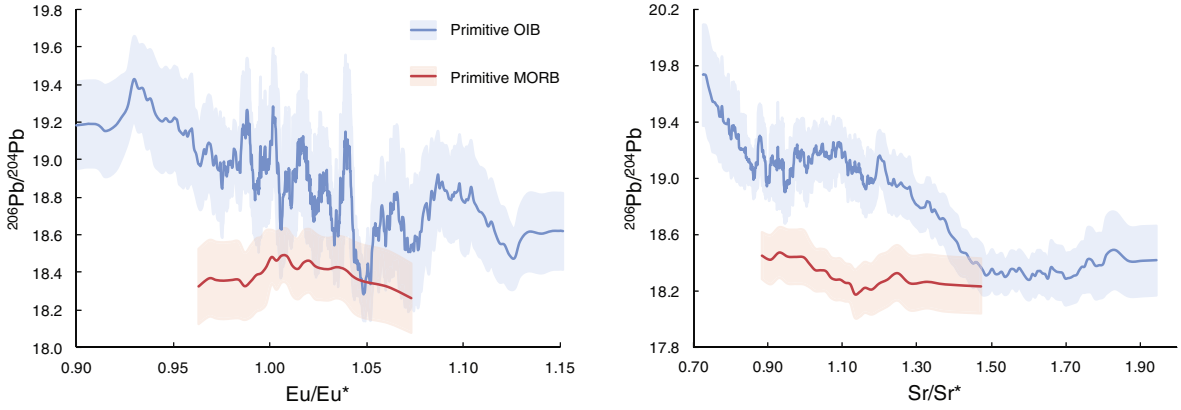

Fig. 7. Running average Pb isotopic composition vs. Eu/Eu* and Sr/Sr* in primitive OIBs (MgO >9 wt.%, $n = 408$) and MORBs (MgO >9 wt.%, $n = 45$). Every 20 samples were averaged to reduce scatter. Note that available high MgO MORB analyses are limited so the Pb isotope-Eu/Eu* and Sr/Sr* correlation remain to be further tested by future studies. Light blue and red shades show the 95% confidence ranges of the average Pb isotopes. OIB data were compiled from GeoRoc and MORB data are from Gale et al. (2013). (For interpretation of the references to colour in this figure legend, the reader is referred to the web version of this article.)

clinopyroxene compositions are only controlled by melting processes unless they experienced metasomatism. According to our model, unmodified peridotitic clinopyroxenes should display negative Eu and Sr anomalies after various degrees of melt depletion.

4.3. Implications for lower crustal recycling in the mantle

Our disequilibrium melting model provides an alternative to recycled lower continental crust to explain the positive Eu and Sr anomalies in primitive MOBRs, and such kinetic effect must be taken into account when evaluating Eu and Sr excess in the mantle source. In addition to positive Eu and Sr anomalies, recycled lower crustal materials that are plagioclase enriched also have low U/Pb and Th/Pb ratios. Lower crustal recycling thus transports less radiogenic Pb isotopes into the mantle (*e.g.*, Jagoutz and Schmidt, 2013; Tang et al., 2015). In ocean island basalts (OIB) with >9 wt.% MgO, the negative correlations between Eu/Eu*-, Sr/Sr*-Pb isotopes (Fig. 7) suggest that the recycled lower crustal materials are an important component in the source of OIB. A similar conclusion was reached by Willbold and Stracke (2010), who showed the negative correlation between Sr isotopes and Eu/Eu* in OIB. In primitive MORBs, Pb isotopes show no correlations with Eu/Eu* and Sr/Sr*.

5. CONCLUSIONS

High precision and accuracy Eu/Eu* and Sr/Sr* measurements in high MgO (>8.5 wt.%) MORB glasses were conducted to evaluate the potential effect of lower crustal

recycling in the MORB source mantle. Primitive MORBs (defined as MORBs with MgO >9 wt.% here), with no correlations of Eu/Eu^* vs. MgO and Sr/Sr^* vs. MgO, have average $Eu/Eu^* = 1.025 \pm 0.025$ and $Sr/Sr^* = 1.24 \pm 0.09$ ($2\ \sigma_m$). Primitive MORBs show both positive and negative Eu and Sr anomalies, and a positive correlation between Eu/Eu^* and Sr/Sr^*, consistent with previous studies (Niu and O'Hara, 2009; Jenner and O'Neill, 2012a,b).

Model calculations show that kinetic fractionation of Sm–Eu–Gd and Pr–Sr–Nd during partial melting ± melt transportation may produce large variations of Eu/Eu^* and Sr/Sr^* that are positively correlated with each other in partial melts under upper mantle conditions. Because partial melts, compared with the MORB source mantle, tend to be enriched in Eu and Sr over Sm–Gd and Pr–Nd, respectively, the MORB source mantle should have lower Eu/Eu^* and Sr/Sr^* than primitive MORBs.

This study does not exclude the possibility that some recycled lower crustal materials might have been mixed into the MORB source mantle, but the negative correlations between Pb isotopes and Eu, Sr anomalies in OIBs suggest that a significant amount of foundered continental lower crust sank to the deep mantle.

ACKNOWLEDGEMENTS

This work was supported by NSF grant EAR0948549. We thank the Smithsonian Institute for providing the MORB glass samples. Special thanks to Roberta Rudnick for discussions and Yu Huang for help with coding. We also appreciate the critical reviews of Bill White and Albrecht Hofmann, Catherine Chauvel, Yaoling Niu and, which helped us to clarify and strengthen the paper. Editors Stefan Weyer and Marc Norman are thanked for handling this manuscript.

APPENDIX A. SUPPLEMENTARY DATA

Supplementary data associated with this article can be found, in the online version, at http://dx.doi.org/10.1016/j.gca.2016.10.025.

REFERENCES

Aigner-Torres M., Blundy J., Ulmer P. and Pettke T. (2007) Laser ablation ICPMS study of trace element partitioning between plagioclase and basaltic melts: an experimental approach. *Contrib. Mineral. Petrol.* **153**(6), 647–667.

Arevalo R. and McDonough W. F. (2010) Chemical variations and regional diversity observed in MORB. *Chem. Geol.* **271**, 70–85.

Bender J., Langmuir C. and Hanson G. (1984) Petrogenesis of basalt glasses from the Tamayo region, East Pacific Rise. *J. Petrol.* **25**, 213–254.

Bézos A. and Humler E. (2005) The $Fe^{3+}/\Sigma Fe$ ratios of MORB glasses and their implications for mantle melting. *Geochim. Cosmochim. Acta* **69**, 711–725.

Burnham A. D., Berry A. J., Halse H. R., Schofield P. F., Cibin G. and Mosselmans J. F. W. (2015) The oxidation state of europium in silicate melts as a function of oxygen fugacity, composition and temperature. *Chem. Geol.* **411**, 248–259.

Cherniak D. J. and Liang Y. (2007) Rare earth element diffusion in natural enstatite. *Geochim. Cosmochim. Acta* **71**, 1324–1340.

Cottrell E. and Kelley K. A. (2013) Redox heterogeneity in mid-ocean ridge basalts as a function of mantle source. *Science* **340**, 1314–1317.

Crowley J. W., Katz R. F., Huybers P., Langmuir C. H. and Park S.-H. (2015) Glacial cycles drive variations in the production of oceanic crust. *Science* **347**, 1237–1240.

Frost D. J. and McCammon C. A. (2008) The redox state of Earth's mantle. *Annu. Rev. Earth Planet. Sci.* **36**, 389–420.

Gale A., Dalton C. A., Langmuir C. H., Su Y. and Schilling J.-G. (2013) The mean composition of ocean ridge basalts. *Geochem. Geophys. Geosyst.* **14**, 489–518.

Jagoutz O. and Schmidt M. W. (2013) The composition of the foundered complement to the continental crust and a re-evaluation of fluxes in arcs. *Earth Planet. Sci. Lett.* **371–372**, 177–190.

Jenner F. E. and O'Neill H. S. C. (2012a) Analysis of 60 elements in 616 ocean floor basaltic glasses. *Geochem. Geophys. Geosyst.* **13**, Q02005.

Jenner F. E. and O'Neill H. S. C. (2012b) Major and trace analysis of basaltic glasses by laser-ablation ICP-MS. *Geochem. Geophys. Geosyst.* **13**, Q03003.

Jull M. and McKenzie D. (1996) The effect of deglaciation on mantle melting beneath Iceland. *J. Geophys. Res. Solid Earth* **101**, 21815–21828.

Lambart S., Laporte D. and Schiano P. (2013) Markers of the pyroxenite contribution in the major-element compositions of oceanic basalts: review of the experimental constraints. *Lithos* **160–161**, 14–36.

Laubier M., Grove T. L. and Langmuir C. H. (2014) Trace element mineral/melt partitioning for basaltic and basaltic andesitic melts: An experimental and laser ICP-MS study with application to the oxidation state of mantle source regions. *Earth Planet. Sci. Lett.* **392**, 265–278.

Liu Y., Hu Z., Gao S., Günther D., Xu J., Gao C. and Chen H. (2008) In situ analysis of major and trace elements of anhydrous minerals by LA-ICP-MS without applying an internal standard. *Chem. Geol.* **257**, 34–43.

Niu Y. (1997) Mantle melting and melt extraction processes beneath ocean ridges: evidence from abyssal peridotites. *J. Petrol.* **38**, 1047–1074.

Niu Y. and O'Hara M. J. (2009) MORB mantle hosts the missing Eu (Sr, Nb, Ta and Ti) in the continental crust: New perspectives on crustal growth, crust–mantle differentiation and chemical structure of oceanic upper mantle. *Lithos* **112**, 1–17.

Niu Y., Waggoner D. G., Sinton J. M. and Mahoney J. J. (1996) Mantle source heterogeneity and melting processes beneath seafloor spreading centers: The East Pacific Rise, 18°–19°S. *J. Geophys. Res. Solid Earth* **101**, 27711–27733.

Niu, Y., Gilmore, T., Mackie, S., Greig, A. and Bach, W. (2002) Mineral chemistry, whole-rock compositions, and petrogenesis of Leg 176 gabbros: data and discussion. In *Proceedings of the Ocean Drilling Program, Scientific Results*, pp. 1–60.

Plank T., Spiegelman M., Langmuir C. H. and Forsyth D. W. (1995) The meaning of "mean F": Clarifying the mean extent of melting at ocean ridges. *J. Geophys. Res. Solid Earth* **100**, 15045–15052.

Qin Z. (1992) Disequilibrium partial melting model and its implications for trace element fractionations during mantle melting. *Earth Planet. Sci. Lett.* **112**, 75–90.

Rudnick R. L. and Gao S. (2014) 4.1 – composition of the continental crust. In *Treatise on Geochemistry (Second Edition)* (eds. H. D. Holland and K. K. Turekian). Elsevier, Oxford, pp. 1–51.

Schreiber H. D. (1986) Redox processes in glass-forming melts. *J. Non-Cryst. Solids* **84**, 129–141.

Shannon R. D. (1976) Revised effective ionic radii and systematic studies of interatomic distances in halides and chalcogenides. *Acta Crystallogr. Sect. A: Crystal Phys. Diffr. Theor. Gen. Crystallogr.* **32**, 751–767.

Sneeringer M., Hart S. R. and Shimizu N. (1984) Strontium and samarium diffusion in diopside. *Geochim. Cosmochim. Acta* **48**, 1589–1608.

Sobolev A. V., Hofmann A. W., Sobolev S. V. and Nikogosian I. K. (2005) An olivine-free mantle source of Hawaiian shield basalts. *Nature* **434**, 590–597.

Sobolev A. V., Hofmann A. W., Kuzmin D. V., Yaxley G. M., Arndt N. T., Chung S.-L., Danyushevsky L. V., Elliott T., Frey F. A., Garcia M. O., Gurenko A. A., Kamenetsky V. S., Kerr A. C., Krivolutskaya N. A., Matvienkov V. V., Nikogosian I. K., Rocholl A., Sigurdsson I. A., Sushchevskaya N. M. and Teklay M. (2007) The amount of recycled crust in sources of mantle-derived melts. *Science* **316**, 412–417.

Sun S.-S. and McDonough W. F. (1989) Chemical and isotopic systematics of oceanic basalts: implications for mantle composition and processes. *Geol. Soc. Lond. Spec. Publ.* **42**, 313–345.

Sun C.-O., Richard J. W. and Sun S.-S. (1974) Distribution coefficients of Eu and Sr for plagioclase-liquid and clinopyroxene-liquid equilibria in oceanic ridge basalt: an experimental study. *Geochim. Cosmochim. Acta* **38**, 1415–1433.

Tang M., McDonough W. F. and Arevalo R. J. (2014) High-precision measurement of Eu/Eu* in geological glasses via LA-ICP-MS analysis. *J. Anal. At. Spectrom.* **29**, 1835–1843.

Tang M., Rudnick R. L., McDonough W. F., Gaschnig R. M. and Huang Y. (2015) Europium anomalies constrain the mass of recycled lower continental crust. *Geology* **43**, 703–706.

Van Orman J., Grove T. and Shimizu N. (2001) Rare earth element diffusion in diopside: influence of temperature, pressure, and ionic radius, and an elastic model for diffusion in silicates. *Contrib. Mineral. Petrol.* **141**, 687–703.

Wanless V. D. and Shaw A. M. (2012) Lower crustal crystallization and melt evolution at mid-ocean ridges. *Nat. Geosci.* **5**, 651–655.

Willbold M. and Stracke A. (2010) Formation of enriched mantle components by recycling of upper and lower continental crust. *Chem. Geol.* **276**, 188–197.

Associate editor: Stefan Weyer